ISSN: 2577 - 8005

Research Article

Medical & Clinical Research

Detailed Study of HPRT1 Gross Deletions Found in 10 Italian Lesch-Nyhan Families

Paola Cattelan, Daniela Segat, Maria Vittoria Enzo, Uros Hladnik and Paola de Gemmis*

Genetics Unit, "Mauro Baschirotto" Institute for Rare Diseases - B.I.R.D. n.p.o. Via B. Bizio, 1 - 36023 Costozza di Longare (Vicenza) - Italy

***Corresponding author**

Paola de Gemmis, Genetics Unit, "Mauro Baschirotto" Institute for Rare Diseases - B.I.R.D. n.p.o. Via B. Bizio, 1 - 36023 Costozza di Longare (Vicenza) - Italy

Submitted: 24 May 2021; **Accepted**: 31 May 2021; **Published**: 10 Jun 2021

Citation: *Paola Cattelan, Daniela Segat, Maria Vittoria Enzo, Uros Hladnik and Paola de Gemmis (2021) Detailed Study of HPRT1 Gross Deletions Found in 10 Italian Lesch-Nyhan Families. Medical & Clinical Research 6(6): 586-591.*

Abstract

Background: *Lesch-Nyhan disease (LND) is an X-linked rare pathology involving the purine nucleotides salvage pathway. Its incidence is estimated in 1:350.000 born. The condition is due to mutations in the HPRT1 (hypoxanthine phosphoribosyl transferase 1) gene of which in our cohort 28% (10/35) are large deletions. In order to better assess the nature of the observed deletions in our LND population we analyzed 10 families carrying large deletions in the HPRT1 gene region and studied the underlying pathogenic mechanisms.*

Methods: *We performed PCR based localization of the break points and sequenced the gap-junction fragments. Bioinformatics analysis was performed through several web tools on the 5' and 3' break points to determine the factors involved in the deletion mechanism.*

Results: *We precisely mapped 10 unique large deletions involving the HPRT1 gene region that span from 300 bp to 64 kbp. No common breakpoints were found and each deletion appears to be family specific.*

Conclusions: *The deletions in the HPRT1 gene area are consistent with the Micro homology-Mediated Break-Induced Replication (MMBIR) mechanism. There are strong links with Alu-s and no recurrent break points with all of the observed deletions being unique. The relatively large amount of deletions in the HPRT1 region is peculiar and linked with the almost absolute lack of polymorphic sites in the HPRT1 gene making it a very interesting region for further studies.*

Keywords: Lesch-Nyhan Disease, HPRT1 Gene, Deletion, Breakpoints, Alu, FoSTeS, MMBIR

Abbreviations:

LND: Lesch-Nyhan Disease
HPRT1: Hypoxanthine Phosphoribosyl Transferase 1
HGprt: Hypoxanthine-Guanine Phosphoribosyl Transferase
IMP: Inosine Monophosphate
GMP: Guanosine Monophosphate
gDNA: Genomic DNA
VDJ: Variable (V) Diversity (D), and Joining (J)
QGRS: Quadruplex Forming G-rich Sequences
MMBIR: Microhomology-Mediated Break-Induced Replication

Introduction

Lesch-Nyhan disease (LND, OMIM 300322) is an X-linked rare purine nucleotides salvage pathway disease. It is characterized by a motor dysfunction, cognitive and behavioral disturbances, and uric acid overproduction. The most common presenting features, hypotonia and developmental delay, are evident by age three to six months. In the classical form of LND, hypotonia is often present since birth and it is therefore a rare cause of floppy infant syndrome. The pathognomonic sign of the classical LND usually develops in early childhood, it is the so called Lesch-Nyhan behavior, a compulsive and subconscious urge towards self-injurious behavior (biting the fingers, hands, lips, and cheeks; banging the head or limbs). Another important part of the LND is the overproduction of uric acid that leads to hyperuricemia, uric acid nephrolithiasis, tophi, and gouty arthritis. Variants of the classical LND with less severe manifestations include hyperuricemia with neurologic dysfunction but no self-injurious behavior and isolated hyperuricemia without marked neurological signs [1-5].

HPRT1 (hypoxanthine phosphoribosyl transferase 1) is the only gene known to be associated with LND. It encodes the hypoxanthine-guanine phosphoribosyl transferase (HGprt) enzyme that primarily converts hypoxanthine to inosine monophosphate (IMP) and guanine to guanosine monophosphate (GMP). Its deficiency leads to accumulation of purines that are converted to xanthine and ultimately to uric acid causing hyperuricemia [6-8].

We have previously published our cohort of 45 patients from 35 unrelated families and determined the genetic cause of the disease in all the cases [9]. We now follow up with the breakpoint analysis of ten cases with gross deletions identified in our laboratories: eight cases were already present in the previous publication but without a proper determination of the extension of the deletions, two cases were not previously described.

The characterization of the precise breakpoints is fundamental for the better understanding of the underlying mechanics and for an optimal assessment of the methods to be used in the LND molecular diagnosis.

Subjects and Methods

Studied Families: We included in this study 10 of the 12 families detected carrying large deletions of the HPRT1 gene. The two excluded families were not available for participation in this study. Informed consent was obtained for all the families and the experiments performed did not require the collection of additional biological material specific for this research. The affected members of all the families presented the classical form of LND. All the initial PCR based gross determinations of the breakpoints were performed on affected males during diagnostic HPRT1 DNA testing.

DNA Isolation, PCR Amplification and Sanger Sequencing of the HPRT1 Gene

Genomic DNA (gDNA) was extracted from peripheral blood using the Nucleospin Blood kit (Mackerey-Nagel, GmbH&Co, Germany) according to the manufacturer instructions. For each patient, the nine exons encoding the entire HPRT1 gene and the corresponding periexonic flanking regions were amplified using primers and conditions as previously described, gDNA analysis was performed as previously published [9, 10].

PCR Based Gross Determination of the Deleted Region

Due to the hemizygous state of the deletions in affected males, the presence or absence of the allele was established by conventional PCR followed by electrophoresis on agarose gel. In all reactions was also included a wild type control to confirm the successful amplification. 93 primer pairs flanking the missing exons at roughly 2 Kb intervals were designed with Primer Blast [11]. All primer pairs were designed to maximize their specificity and trying to maintain the size of the amplicons between 100 and 500 bases.

Breakpoint Fine Mapping and Junction Fragment Sequencing

After determining the closest primer pairs outside the deleted region, we amplified the junction fragments initially using the forward primer of the most 5' primer pair before the deletion and the reverse primer of the most 3' primer pair after the deletion. The resulting amplicons were obtained adjusting the PCR mixture containing Taq Gold 360 (Thermo Fisher Scientific, Massachusetts, USA) with betaine 10% or with DMSO 10% in addition to betaine 10% for the more difficult amplifications. The reaction used was a Touchdown PCR from 70° to 54°C and PCR conditions were set to 1 min denaturation, 1 min annealing of primers and 1 to 2 min extension for 40 cycles. 100ng of DNA were used for each amplification reaction.

Once verified the presence of PCR products by 2% agarose gel analysis, the amplicons were purified by DNA Clean & Concentrator-25 kit (Zymoresearch, Irvine, USA) and sequenced on an ABI PRISM® 3130 Genetic Analyzer sequencer. The sequences were aligned with the reference sequence of the region using the UCSC Blat program, determining in this way the precise position of the breakpoints, the dimension of the resulting deletions and eventual insertions [12]. According to the HGVS guidelines, in the cases of homology at the breakpoints, the breakpoint position was always determined to be the most 5' base, all subsequent analyses took in account the possible alternative positions of the breakpoints.

Bioinformatics Sequence Analysis of the Deletion Breakpoints Region

In total we analyzed 10 large deletions of HPRT1 with a precise localization of the breakpoints. All breakpoint descriptions are reported with the coordinates of UCSC genome browser build GRCh38. Location and data analyses from all patients were compiled in a Microsoft Excel spreadsheet, breakpoint locations were uploaded and displayed in UCSC (Figure 1) [13]. We used various online bioinformatics tools (see the section Web Resources) to study the deletion events.

The exact positions of the proximal and distal breakpoints were confirmed using BLAT from UCSC Genome Browser Website with the junction fragment as the query sequence. Breakpoints represent the boundaries of the deleted DNA region, while the genomic segments surrounding each breakpoint and comprising both the deleted and the non-deleted segments are defined as "breakpoint regions". Reference genomic sequences were obtained from UCSC on the basis of breakpoint positions. CLUSTALW was used to align the junction fragment with the reference genomic sequence from both the proximal and distal breakpoint regions. We used Blastn to search for sequence homologies, considering genomic segments of a length of 400 bp centered both on the DNA breakpoints and the junction fragment. Additionally, these 400bp sequences were also scanned searching for repetitive elements (core, similcore, Alu, SINE, LINE, etc), and for sequence motifs frequently associated to DNA rearrangements and breakpoints formation such as translin binding site, human deletion hotspot, DNA polymerase arrest site, DNA polymerase A frameshift, DNA polymerase B frameshift, Polymerase A/B frameshift hotspot 1, Polymerase A/B frameshift hotspot 2, VDJ (Variable (V) diversity (D), and Joining (J)) genes recombinase nonamere consensus, QGRS (Quadruplex forming G-rich Sequences), Chi line sequence, palindromic sequences, topoisomerase binding sites [14-16].

Refined computer-based sequence analysis included the screening for tandem and palindromic inverted repeats in a 400 bp breakpoint

regions was performed using Tandem Repeats Finder. Perfect uninterrupted tracts of purine and pyrimidine repeats ≥10 bp were identified using Word processor software. For each deletion we searched for the presence of the 26 bp core consensus sequence at the 5' end of *Alu* elements at the breakpoints (±2000 bp) and at the junction site [17].

Finally we used Mfold 3.5 to predict secondary structures, analyzing a region of 30 bp both for the breakpoints and the junction fragment comparing their relative stability.

Results

In our 10 families the initial suspect of a deletion derived by the absence of the PCR product from one or more of the HPRT1 gene exons in affected males. Additional primer pairs were therefore designed and amplified by PCR in order to roughly determine the dimension of the deleted region. The closest successfully amplified PCR products were sequenced to confirm their positioning and the external two primers were used to obtain the junction fragment.

The junction fragments obtained were aligned on the NC_000023.11 and nomenclated according to the current HGVS guidelines as seen in Table 1 [18].

Table 1: List of HPRT1 Deletions Defined In This Study

Family	Involved exons (introns)	Deletion size	Deletion localization on chromosome X [NC_000023.11]	Deletion according to the HPRT1 gene [NM_000194.2]
1	E1-E3	37039	g.134440277_134477315delins195	c.1-167-19869_318+1952delins195
2	E1-E9	67477	g.134454846_134522322del	c.1-167-5300_*591+21655del
3	E3-E9	68061	g.134473554_134541614del	c.134+88_*591+40947del
4	E2-E9	41832	g.134472449_134514280del	c.28-911_*591+13613del
5	E4	4031	g.134483589_134487619del	c.319-2877_384+1090del
6	(I8)	726	g.134499290_134500015del	c.609+605_610-14del
7	E2	4480	g.134469689_134474168del	c.28-3671_134+704del
8	E4	29	g.134486461_134486489del	c.319-5_343del
9	E4	2512	g.134485851_134488362del	c.319-615_385-1825del
10	E4-E5	7213	g.134485917_134493129del	c.319-549_403-378del

For each patient the position of the proximal (BP5) and the distal (BP3) breakpoint, deletion's extension and eventual insertions at the junction site are reported. The precise determination of the breakpoints is determined by the HGVS guidelines as the 3' most position of the uncertainty range. Deletions varied in size from 29 to 68061 nucleotides.

In family 1 the deletion spanned the first 3 exons of the HPRT1 gene, ranging from 19869 nucleotides 5' of the HPRT1 gene to nucleotide 1952 of intron 3. In total the deletion was spanning 37039 nucleotides and contained an insertion of 195 bases of which 192 bases were identical to the sequence on the complementary strand of DNA in positions from 134441066 to 134440875 5' of the HPRT1 gene, 599 bases from the 5' breakpoint. For the remaining three nucleotides (TTA) no clear origin could be determined. There is a 4 nucleotide microhomology between the 5' breakpoint and the 5' of the insertion; no homology could be detected between the 3' portion of the insertion and the 3' breakpoint. The TTA sequence could not be reliably linked to any specific genomic location by using the adjacent sequences as seen in the patient's DNA.

In family 2 the deletion involved the entire HPRT1 gene, ranging from 5300 nucleotides 5' of the HPRT1 gene to 21655 nucleotides 5' of it. In total the deletion was spanning 67477 nucleotides. There is a region of 21 nucleotides of perfect homology between the 5' and 3' breakpoints.

In family 3 the deletion spanned from the nucleotide 88 of intron 2 to 40947 nucleotides after the HPRT1 gene. In total the deletion was spanning 68061 nucleotides, a microhomology of three nucleotides was present at the breakpoints. The deletion included also the MIR450B, MIR450A1, MIR450A2 and MIR542 microRNAs (miRNAs). miRNAs are 20-24 nucleotide long non-coding RNAs that regulate gene expression by affecting both the stability and translation of mRNAs [19, 20].

In family 4 the deletion spanned from the nucleotide -911 of intron 1 to 13613 nucleotides after the HPRT1 gene. In total the deletion was spanning 41832 nucleotides, a microhomology of two nucleotides was present at the breakpoints.

In family 5 the deletion spanned from the nucleotide -2877 of intron 3 to nucleotide 1090 of intron 4 of the HPRT1 gene. In total the deletion was spanning 4031 nucleotides.

In family 6 the deletion spanned from the nucleotide 605 to nucleotide -14 of intron 8 of the HPRT1 gene. In total the deletion was spanning 726 nucleotides, a microhomology of four nucleotides was present at the breakpoints.

In family 7 the deletion spanned from the nucleotide -3671 of intron 1 to nucleotide 704 of intron 2 of the HPRT1 gene. In total the deletion was spanning 4480 nucleotides, a microhomology of

two nucleotides was present at the breakpoints.

In family 8 the deletion spanned from the nucleotide -5 of intron 3 to nucleotide c.343 of the HPRT1 gene. In total the deletion was spanning 29 nucleotides, a microhomology of three nucleotides was present at the breakpoints.

In family 9 the deletion spanned from the nucleotide -615 of intron 3 to nucleotide -1833 of intron 4 of the HPRT1 gene. In total the deletion was spanning 2512 nucleotides.

In family 10 the deletion spanned from the nucleotide -547 of intron 3 to nucleotide -378 of intron 5 of the HPRT1 gene. In total the deletion was spanning 7213 nucleotides, a microhomology of three nucleotides was present at the breakpoints.

Discussion

The observed deletions vary substantially in size and in location and span not only the whole HPRT1 gene region but extend to a wider area of chromosome X as can be seen in Figure 1. No apparent hot spots for deletion emerged from our study but there appears to be a higher incidence of 5' breakpoints in intron 3.

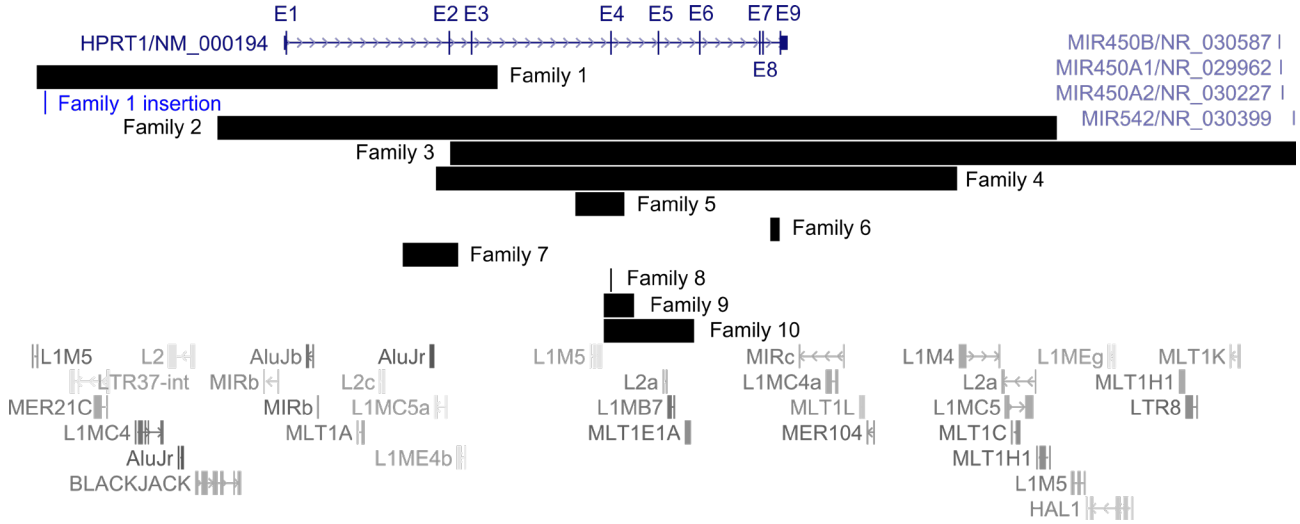

Figure 1: Localization of HPRT1 deletions on chromosome Xq26.2 - Xq26.3 (NC_000023.10: 134,440,000-134,542,750).

The segments at the top represent the location of the HPRT1 gene exons 1 to 9 (E1 to E9). Black bars (Family 1- Family 10) represent deleted regions in each family. Family 1 insertion denotes the origin on the complementary strand of 192 nucleotides of the insertion in family 1 (192/195 nucleotides). The location of the miRNA genes MIR450B, MIR450A1, MIR450A2 and MIR542 is visible on the right top part of the image. The bottom part of the image shows the locations of the major interrupted repeats joined by Repeat Masker in the region. Taken from UCSC genome browser and modified maintaining the scale and position of the displayed elements.

The extension of the deletion size ranged from 29b to ~68 kb. Proximal breakpoints are scattered throughout a ~59 kb region, while distal breakpoints lie in a ~67 kb interval. There seems to be no shared overlapping regions between the deletions. No evidence of deletion hot spots was found by aligning the breakpoint localizations, however some grouping of proximal or distal breakpoints can be observed in Figure 1: in particular, family 9 and 10 have the 5' breakpoint within 67 bases with family 8 having the 5' breakpoint 610 bases downstream. Families 3 and 4 have their 5' breakpoints within a region of 1106 bases.

In relation to the HPRT1 gene, two of the 5' breakpoints are located upstream from the gene, two in intron 1, one in intron 2 where is located also one of the 3' breakpoints. The biggest number of 5' breakpoints are in intron 3 where four of them are located together with one 3' breakpoint. Only one of the breakpoints is located within an exon, more precisely a 3' breakpoint situated in exon 4. Intron 4 contains two 3' breakpoints and intron 5 one. Intron 8 contains both the breakpoints of the deletion in family 8. Finally, three of the 3' breakpoints are located downstream from the HPRT1 gene.

Of the ten deletions, four involved just one exon, one deletion involved the whole HPRT1 gene while a deletion included only 726 bp of intron 8. The other deletions identified involved 2, 3, 7 or 8 exons.

Only the deletion in family 1 had also an insertion of 195 nucleotides. Of these, 192 nucleotides derive from the complementary strand in close proximity to the 5' breakpoint (599 nucleotides 3' of the actual breakpoint), while the origin of the remaining three nucleotides is unclear and they could be linked to the repair mechanisms involved or an additional template switch.

The deletion in family 3 was initially described as a deletion of the exons from 2 to 9 as described by missing exon amplification in our 2010 review, but it was actually confirmed that the deletion starts in intron 3 in position c.134+88 and therefore it does not involve exon 2 [9]. The deletion in family 3 is also the only observed deletion that directly includes additional known genes, namely the miRNA genes MIR450B, MIR450A1, MIR450A2 and MIR542. These are considered to be involved in DNA damage response. Diseases associated with MIR450A1 include also the

hyperlucent lung. Diseases associated with MIR542 include lymphoplasmacytic lymphoma and leiomyoma. Several other neoplastic diseases are linked with these miRNAs [19, 20].

The affected male in family 3 has a classical form of LND with the peculiarity of an extremely early kidney failure in the neonatal period that required a kidney transplant. Considering the linkage between miRNAs and kidney disease it is plausible that the deletion of the four miRNAs observed might have been a major contributing cause to the kidney problem. In this case, the kidney transplant from a healthy donor might have been the best possible solution, bypassing also the missing miRNA problem.

The regions of the deletion breakpoints are characterized by the presence of repeated, low complexity sequences associated with the formation of deletions. Only in the case of family 8 no specific low complexity regions could be identified in direct proximity of the breakpoints.

In conclusion, all the identified deletions appear to be restricted to single families and no repeated location for the breakpoints was found in line with the previously published deletions [21-27]. The mutations appear to be therefore nonrecurrent and following either the microhomology-mediated break-induced replication (MMBIR) model or the fork stalling and template switching (FoSTeS) model [28-33].

It is always important to remember, when studying deletions, that the sequence changes we see might not be the actual locations where the deletion originated. The actual deletion could have happened due to an error considerably distant from the apparent breakpoint with a homologous sequence deriving from a different template or repair mechanisms masking this. In a similar fashion, a deletion could actually consist of several distinct template switches that do not appear evident due to sequence homology between the different templates or repair mechanisms.

The identification of a relatively large amount of deletions in the HPRT1 region is peculiar and linked with the almost absolute lack of polymorphic sites in the HPRT1 gene. It will allow accurate carrier detection and helpful information for patients' families' genetic counseling.

Acknowledgments

We thank the patients and their families as well as the medical doctors and other professionals that referred the families to our institute.

References

1. Torres RJ, Puig JG (2007) Hypoxanthine-guanine phosphoribosyltransferase (HPRT) deficiency: Lesch–Nyhan syndrome. Orphanet J Rare Dis 2: 48.
2. Jinnah HA, Visser JE, Harris JC, Verdu A, Larovere L, et al. (2006) Lesch–Nyhan Disease International Study Group. Delineation of the motor disorder of Lesch–Nyhan disease. Brain 129: 1201–1217.
3. http://www.orpha.net
4. http://www.lesch-nyhan.org
5. Schretlen DJ, Ward J, Meyer SM, Yun J, Puig JG, et al. (2005) Behavioral aspects of Lesch-Nyhan disease and its variants. Dev Med Child Neurol 47: 673–7.
6. Fu R, Sutcliffe D, Zhao H, Huang X, Schretlen DJ, Benkovic S, Jinnah HA (2015) Clinical severity in Lesch-Nyhan disease: the role of residual enzyme and compensatory pathways. Mol Genet Metab 114: 55–61.
7. Fu R, Ceballos-Picot I, Torres RJ, Larovere LE, Yamada Y, et al (2014) Genotype-phenotype correlations in neurogenetics: Lesch-Nyhan disease as a model disorder. Brain 137: 1282–303.
8. Göttle M, Prudente CN, Fu R, Sutcliffe D, Pang H, et al. (2014) Loss of neurotransmitter phenotype among midbrain dopamine neurons in Lesch-Nyhan disease. Ann Neurol 76: 95–107.
9. de Gemmis P, Anesi L, Lorenzetto E, Gioachini I, Fortunati E, et al. (2010) Analysis of the HPRT1 gene in 35 Italian Lesch-Nyhan families: 45 patients and 77 potential female carriers. Mutat Res 692: 1-5.
10. Hladnik U, Nyhan WL, Bertelli M (2008) Variable expression of HPRT deficiency in 5 members of a family with the same mutation. Arch Neurol 65: 1240–1243.
11. Ye J, Coulouris G, Zaretskaya I, Cutcutache I, Rozen S, et al. (2012) Primer-BLAST: A tool to design target-specific primers for polymerase chain reaction. BMC Bioinformatics 13: 134.
12. BLAT: Kent WJ (2002) BLAT - the BLAST-like alignment tool. Genome Res 12: 656-64.
13. Kent WJ, Sugnet CW, Furey TS, Roskin KM, Pringle TH, et al. (2002) The human genome browser at UCSC. Genome Res 12: 996-1006.
14. Gu W, Zhang F, Lupski JR (2008) Mechanisms for human genomic rearrangements. Patho Genetics 1: 4.
15. Lupski JR, Stankiewicz P, Lupski JR, Stankiewicz P (2005) Genomic disorders: molecular mechanisms for rearrangements and conveyed phenotypes. PLoS Genet 1: e49.
16. Lupski JR (1998) Genomic disorders: structural features of the genome can lead to DNA rearrangements and human disease traits. Trends Genet 14: 417-22.
17. Deininger P (2011) Alu elements: know the SINEs. Genome Biol. 12: 236.
18. den Dunnen JT (2017) Describing Sequence Variants Using HGVS Nomenclature. Methods Mol Biol. 1492: 243-251.
19. Wei Q, Mi QS, Dong Z (2013) The regulation and function of microRNAs in kidney diseases. IUBMB Life. 65: 602-14.
20. Chandrasekaran K, Karolina DS, Sepramaniam S, Armugam A, Wintour EM, et al. (2012) Role of microRNAs in kidney homeostasis and disease. Kidney Int 81: 617-27.
21. Gibbs RA, Nguyen PN, Edwards A, Civitello AB, Caskey CT (1990) Multiplex DNA deletion detection and exon sequencing of the hypoxanthine phosphoribosyltransferase gene in Lesch–Nyhan families. Genomics 7: 235–244.
22. Wehnert M, Herrmann FH (1990) Characterization of three new deletions at the 5'end of the HPRT structural gene. J. Inherit. Metab. Dis. 13: 178–183.
23. Tvrdik T, Marcus S, Hou SM, Fält S, Noori P, et al. (1998) Molecular characterization of two deletion events involving Alu-sequences, one novel base substitution and two tentative hotspot mutations in the hypoxanthine phosphoribosyltransferase (HPRT) gene in five patients with

Lesch-Nyhan syndrome. Hum Genet 103: 311-8.
24. Mizunuma M, Fujimori S, Ogino H, Ueno T, Inoue H, et al. (2001) A recurrent large Alu-mediated deletion in the hypoxanthine phosphoribosyltransferase (HPRT1) gene associated with Lesch-Nyhan syndrome. Hum Mutat 18: 435-43.
25. Brooks EM, Branda RF, Nicklas JA, O'Neill JP (2001) Molecular description of three macro-deletions and an Alu-Alu recombination-mediated duplication in the HPRT gene in four patients with Lesch-Nyhan disease. Mutat Res 476: 43-54.
26. Cho JH, Choi JH, Heo SH, Kim GH, Yum MS, et al. (2019) Phenotypic and molecular spectrum of Korean patients with Lesch-Nyhan syndrome and attenuated clinical variants. Metab Brain Dis 34: 1335-1340.
27. Taniguchi A, Yamada Y, Hakoda M, Sekita C, Kawamoto M, et al. (2011) Molecular characterization of a deletion in the HPRT1 gene in a patient with Lesch-Nyhan syndrome. Nucleosides Nucleotides Nucleic Acids. 30: 1266-71.
28. Lee JA, Carvalho CM, Lupski JR (2007) A DNA replication mechanism for generating nonrecurrent rearrangements associated with genomic disorders. Cell 131: 1235-47.
29. Carvalho CM, Lupski JR (2016) Mechanisms underlying structural variant formation in genomic disorders. Nat Rev Genet. 17: 224-38.
30. Anesi L, de Gemmis P, Galla D, Hladnik U (2012) Two new large deletions of the AVPR2 gene causing nephrogenic diabetes insipidus and a review of previously published deletions. Nephrol Dial Transplant. 27: 3705-12.
31. Gu W, Zhang F, Lupski JR (2008) Mechanisms for human genomic rearrangements. Pathogenetics. 1: 4.
32. Koumbaris G, Hatzisevastou-Loukidou H, Alexandrou A, Ioannides M, Christodoulou C, et al. (2011) FoSTeS, MMBIR and NAHR at the human proximal Xp region and the mechanisms of human Xq isochromosome formation. Hum Mol Genet. 20: 1925-36.
33. Zhang F, Khajavi M, Connolly AM, Towne CF, Batish SD, et al. (2009) The DNA replication FoSTeS/MMBIR mechanism can generate genomic, genic and exonic complex rearrangements in humans. Nat Genet 41: 849-53.